NASA TECHNICAL NOTE

NASA TN D-7888

NASA TN D-7888

SUPERSONIC FLUTTER OF PANELS LOADED WITH INPLANE SHEAR

James Wayne Sawyer

Langley Research Center

Hampton, Va. 23665

NATIONAL AERONAUTICS AND SPACE ADMINISTRATION • WASHINGTON, D. C. • APRIL 1975

1. Report No.	2. Government Accession No.	3. Recipient's Catalog No.
NASA TN D-7888		

4. Title and Subtitle	5. Report Date
SUPERSONIC FLUTTER OF PANELS LOADED WITH INPLANE SHEAR	April 1975
	6. Performing Organization Code

7. Author(s)	8. Performing Organization Report No.
James Wayne Sawyer	L-9908
	10. Work Unit No.
9. Performing Organization Name and Address	506-17-22-01
NASA Langley Research Center Hampton, Va. 23665	11. Contract or Grant No.
	13. Type of Report and Period Covered
12. Sponsoring Agency Name and Address	Technical Note
National Aeronautics and Space Administration Washington, D.C. 20546	14. Sponsoring Agency Code

15. Supplementary Notes

16. Abstract

A modal flutter analysis for biaxially loaded, orthotropic panels, using linear piston-theory aerodynamics, has been extended in order to include the effects of inplane shear loading. Flutter boundaries for shear loads up to buckling are calculated for simply supported, isotropic panels of various length-width ratios and for a square, isotropic panel with elastic boundary conditions along the leading and trailing edges. These flutter boundaries are used to define conservative design curves. Sample calculations made using these design curves indicate that practical panels, which have otherwise been adequately designed, could become flutter critical if the inplane shear loads approach the buckling value.

17. Key Words (Suggested by Author(s))	18. Distribution Statement
Panel flutter Elastic supports Inplane shear	Unclassified – Unlimited New Subject Category 39

19. Security Classif. (of this report)	20. Security Classif. (of this page)	21. No. of Pages	22. Price*
Unclassified	Unclassified	31	$3.75

*For sale by the National Technical Information Service, Springfield, Virginia 22151

SUPERSONIC FLUTTER OF PANELS LOADED WITH INPLANE SHEAR

James Wayne Sawyer
Langley Research Center

SUMMARY

A modal flutter analysis for biaxially loaded, orthotropic panels, using linear piston-theory aerodynamics, has been extended in order to include the effects of inplane shear loading. Flutter boundaries for shear loads up to buckling are calculated for simply supported, isotropic panels of various length-width ratios and for a square, isotropic panel with elastic boundary conditions along the leading and trailing edges. For the simply supported panels, the shear loading is shown to have a large destabilizing effect when the buckling load is approached. For such cases, the degradation in flutter resistance is comparable to that exhibited by panels near buckling caused by biaxial loading. The out-of-plane flexibility of the boundary supports (deflectional springs) at the leading and trailing edges is shown to have a large destabilizing influence on the flutter of unstressed panels, but at the point of buckling the springs may be either stabilizing or destabilizing. The flutter boundaries were used to define conservative design curves. The sample calculations made with these design curves indicate that practical panels, which have otherwise been adequately designed, could become flutter critical if the inplane shear loads approach the buckling value.

INTRODUCTION

Although a large body of flutter data is reported in the literature (see ref. 1), most panel flutter studies have ignored the effects of inplane shear loading. However, with the advent of present day high performance aircraft and reusable space vehicles, new surface structure designs have emerged which utilize shear-strength capability. For example, the large cargo-bay door of the shuttle orbiter is designed to transmit loads through shear. Unfortunately, no experimental data exist on the flutter of panels loaded in inplane shear, and the only analytical study available (see ref. 2) is limited to simply supported, isotropic panels with small length-width ratios. Therefore, an analytical study has been undertaken in order to provide a better understanding of the effects of inplane shear on the flutter of panels. In the present investigation, a modal analysis for the flutter of biaxially loaded, orthotropic panels with flexible supports and using linear piston-theory aerodynamics is

extended to include the effects of inplane shear. Calculations are made for simply supported and spring-supported, isotropic panels with inplane shear loads up to the point of buckling in the presence of airflow. The resulting flutter boundaries are used to define conservative, simple-to-use design curves.

SYMBOLS

Values are given in both SI and U.S. Customary Units. The measurements were made in U.S. Customary Units.

A_{mn} Fourier series coefficients (see eq. (12))

a panel length (x-direction)

b panel width (y-direction)

c free-stream speed of sound

D_x panel bending stiffness in x-direction

D_y panel bending stiffness in y-direction

D_{xy} panel twisting stiffness

D_1 $= \dfrac{D_x}{1 - \mu_x\mu_y}$

D_2 $= \dfrac{D_y}{1 - \mu_x\mu_y}$

D_{12} $= D_{xy} + \mu_x D_2$

E modulus of elasticity of panel material

g_a aerodynamic damping coefficient (see eq. (13e))

g_b bending structural damping coefficient

g_m membrane structural damping coefficient

h panel skin thickness

i	$= \sqrt{-1}$
K_d, K_r, K_t	deflectional, rotational, and torsional spring constants, respectively, per unit length
$\bar{K}_d, \bar{K}_r, \bar{K}_t$	nondimensional deflectional, rotational, and torsional spring constants, respectively (see eqs. (10))
$\bar{K}_{xy}$	$= \frac{N_{xy} a^2}{D_1 \pi^2}$
$\bar{K}_{xy_{bu}}$	value of $\bar{K}_{xy}$ for inplane shear-buckling load in presence of airflow
M	Mach number
m	number of half-waves in x-direction
N_x, N_y	uniform inplane normal loads per unit length in x- and y-direction, respectively
N_{xy}	uniform inplane shear loads per unit length
n	number of half-waves in y-direction
p	see equation (3)
q	dynamic pressure of airstream
r, s	integers
t	time
V	potential energy
w	lateral deflection of panel
w_{mn}	lateral deflection of panel describing shape of natural mode of vibration
X	function describing shape of natural mode of vibration in x-direction

x,y	Cartesian coordinates of panel (see fig. 1)
α	complex frequency
α_{mn}	complex natural frequency
β	compressibility factor, $\sqrt{M^2 - 1}$
γ	panel mass per unit area
η	nondimensional coordinate, y/b
Λ	cross-flow angle
λ	dynamic-pressure parameter, $\frac{2qa^3}{\beta D_1}$
λ_o	dynamic-pressure parameter at flutter for zero stress
μ_x,μ_y	Poisson's ratio in x- and y-direction, respectively
ξ	nondimensional coordinate, x/a
ρ	free-stream air density
ω	frequency
ω_r	fundamental frequency of simply supported beam (radians per sec), $\frac{\pi^2}{a^2}\sqrt{\frac{D_1}{\gamma}}$

Subscripts:

m,r	number of half-waves in x-direction
n,s	number of half-waves in y-direction

ANALYSIS

Governing Equations

A flutter analysis is presented which extends the analysis of reference 3 to include inplane shear loads. Because of the similarity of the two analyses, only equations or

solution procedures which differ from those presented in reference 3 are discussed in detail. The panel and coordinate system shown in figure 1 is for a flat orthotropic panel with a supersonic flow at Mach number M at an arbitrary cross-flow angle over one surface. The panel edges at $x = \pm \frac{a}{2}$ are supported by deflectional, rotational, and torsional springs; the other two edges ($y = 0$, and b) are simply supported. The panel is loaded by uniform inplane normal loads N_x and N_y (positive in compression) and by a uniform inplane shear load N_{xy}. Aerodynamic loading is given by linear piston theory and includes aerodynamic damping. The governing equations can be developed using the virtual work of the system as given by the following equation written in terms of nondimensional orthotropic panel properties. (This equation corresponds to the expression for the first variation of the potential energy in ref. 4):

$$\delta V = ab \int_{-1/2}^{1/2} \int_0^1 \left\{ \frac{\partial^2 w}{\partial \xi^2} \delta\left(\frac{\partial^2 w}{\partial \xi^2}\right) + \frac{\mu_y a^2}{b^2}\left[\frac{\partial^2 w}{\partial \xi^2} \delta\left(\frac{\partial^2 w}{\partial \eta^2}\right) + \frac{\partial^2 w}{\partial \eta^2} \delta\left(\frac{\partial^2 w}{\partial \xi^2}\right)\right] + \frac{D_2}{D_1}\frac{a^4}{b^4} \frac{\partial^2 w}{\partial \eta^2} \delta\left(\frac{\partial^2 w}{\partial \eta^2}\right) \right.$$

$$\left. + \frac{2a^2 D_{xy}}{b^2 D_1} \frac{\partial^2 w}{\partial \xi\, \partial \eta} \delta\left(\frac{\partial^2 w}{\partial \xi\, \partial \eta}\right) \right\} d\xi\, d\eta - \frac{ab}{D_1} \int_{-1/2}^{1/2} \int_0^1 \left\{ a^2 N_x \frac{\partial w}{\partial \xi} \delta\left(\frac{\partial w}{\partial \xi}\right) + \frac{a^4 N_y}{b^2} \frac{\partial w}{\partial \eta} \delta\left(\frac{\partial w}{\partial \eta}\right) \right.$$

$$\left. + \frac{a^3}{b} N_{xy}\left[\frac{\partial w}{\partial \xi} \delta\left(\frac{\partial w}{\partial \eta}\right) + \frac{\partial w}{\partial \eta} \delta\left(\frac{\partial w}{\partial \xi}\right)\right] + \frac{a^4 p}{D_1} \delta w \right\} d\xi\, d\eta + \int_0^1 \left[\frac{2a^2 K_r}{D_1} \frac{\partial w}{\partial \xi} \delta\left(\frac{\partial w}{\partial \xi}\right) \right.$$

$$\left. + \frac{2K_t a^4}{D_1 b^2} \frac{\partial w}{\partial \eta} \delta\left(\frac{\partial w}{\partial \eta}\right) + \frac{2K_d a^4}{D_1} w\, \delta w \right] \Bigg|_{-1/2}^{1/2} b\, d\eta \qquad (1)$$

In equation (1), K_d, K_r, and K_t are the respective deflectional, rotational, and torsional spring constants per unit length;

$$\left.\begin{aligned} D_1 &= \frac{D_x}{1 - \mu_x \mu_y} \\ D_2 &= \frac{D_y}{1 - \mu_x \mu_y} \end{aligned}\right\} \qquad (2)$$

and

$$p = \gamma \frac{\partial^2 w}{\partial t^2} + \rho c \frac{\partial w}{\partial t} + \frac{2q}{\beta a}\left(\cos \Lambda \frac{\partial w}{\partial \xi} + \frac{a}{b} \sin \Lambda \frac{\partial w}{\partial \eta}\right) \qquad (3)$$

After integration by parts equation (1) becomes:

$$\delta V = ab \int_{-1/2}^{1/2} \int_0^1 \left[\frac{\partial^4 w}{\partial \xi^4} + 2\mu_y \frac{a^2}{b^2} \frac{\partial^4 w}{\partial \xi^2 \partial \eta^2} + \frac{D_2}{D_1} \frac{a^4}{b^4} \frac{\partial^4 w}{\partial \eta^4} + \frac{2D_{xy}}{D_1} \frac{a^2}{b^2} \frac{\partial^4 w}{\partial \xi^2 \partial \eta^2} + \frac{N_x a^2}{D_1} \frac{\partial^2 w}{\partial \xi^2} \right.$$

$$+ \frac{N_y a^4}{D_1 b^2} \frac{\partial^2 w}{\partial \eta^2} + \frac{2N_{xy} a^3}{D_1 b} \frac{\partial^2 w}{\partial \xi \partial \eta} + \frac{\gamma a^4}{D_1} \frac{\partial^2 w}{\partial t^2} + \frac{\rho c a^4}{D_1} \frac{\partial w}{\partial t} + \frac{2qa^3}{\beta D_1} \left(\cos \Lambda \frac{\partial w}{\partial \xi} \right.$$

$$\left. \left. + \frac{a}{b} \sin \Lambda \frac{\partial w}{\partial \eta} \right) \right] \delta w \, d\xi \, d\eta + \int_0^1 \left(-a \frac{\partial^3 w}{\partial \xi^3} - \mu_y \frac{a^3}{b^2} \frac{\partial^3 w}{\partial \xi \partial \eta^2} - \frac{2D_{xy}}{D_1} \frac{a^3}{b^2} \frac{\partial^3 w}{\partial \xi \partial \eta^2} - \frac{N_x a^3}{D_1} \frac{\partial w}{\partial \xi} \right.$$

$$\left. - \frac{K_t a^4}{D_1 b^2} \frac{\partial w}{\partial \eta} - \frac{N_{xy}}{D_1} \frac{a^4}{b} \frac{\partial w}{\partial \eta} + \frac{K_d w a^4}{D_1} \right) \delta w \Big|_{-1/2}^{1/2} b \, d\eta + \int_0^1 \left(a^2 \frac{\partial^2 w}{\partial \xi^2} + \mu_y \frac{a^4}{b^2} \frac{\partial^2 w}{\partial \xi^2} \right.$$

$$\left. + \frac{K_r}{D_1} a^3 \frac{\partial w}{\partial \xi} \right) \delta \left(\frac{\partial w}{\partial \xi} \right) \Big|_{-1/2}^{1/2} \frac{b}{a} \, d\eta + \int_{-1/2}^{1/2} \left(-\mu_y \frac{a^2}{b} \frac{\partial^3 w}{\partial \xi^2 \partial \eta} - \frac{D_2}{D_1} \frac{a^4}{b^3} \frac{\partial^3 w}{\partial \eta^3} \right.$$

$$\left. - \frac{2D_{xy}}{D_1} \frac{a^2}{b} \frac{\partial^3 w}{\partial \xi^2 \partial \eta} - \frac{N_y a^4}{D_1 b} \frac{\partial w}{\partial \eta} - \frac{N_{xy}}{D_1} a^3 \frac{\partial w}{\partial \xi} \right) \delta w \Big|_0^1 a \, d\xi$$

$$+ \int_{-1/2}^{1/2} \left(\mu_y a^2 \frac{\partial^2 w}{\partial \xi^2} + \frac{D_2}{D_1} \frac{a^2}{b^2} \frac{\partial^2 w}{\partial \eta^2} \right) \delta \left(\frac{\partial w}{\partial \eta} \right) \Big|_0^1 \frac{a}{b} \, d\xi + \left[\frac{2D_{xy}}{D_1} \frac{a^3}{b} \frac{\partial^2 w}{\partial \xi \partial \eta} \right.$$

$$\left. + \frac{K_t a^4}{D_1 b} \frac{\partial w}{\partial \eta} \right] \delta w \Big|_0^1 \Big|_{-1/2}^{1/2} = 0 \qquad (4)$$

According to the principle of virtual work δV must vanish, and, since δw, $\delta\left(\frac{\partial w}{\partial \xi}\right)$, and $\delta\left(\frac{\partial w}{\partial \eta}\right)$ are independent and generally not zero, the coefficients of these terms must be zero independently. The coefficient in the double integral term set equal to zero is recognized as the governing equation, and the coefficient in the single integral terms set equal to zero is recognized as the boundary conditions.

Vibration Solution

The flutter solution to equation (4) is based on a modal analysis which employs the natural modes and frequencies of the panel. These modes and frequencies can also be obtained directly from equation (4) after setting the aerodynamic pressure q equal to zero and assuming the following form for w:

$$w = w_{mn}e^{\alpha_{mn}t} \tag{5}$$

where α_{mn} is the complex damped natural frequency and w_{mn} is the natural mode shape. Substituting equation (5) into equation (4) gives the following governing equation and boundary conditions:

$$\left(1 + ig_b\right)\left[\frac{\partial^4 w_{mn}}{\partial\xi^4} + 2\,\frac{\mu_y D_1 + D_{xy}}{D_1}\,\frac{a^2}{b^2}\,\frac{\partial^4 w_{mn}}{\partial\xi^2\,\partial\eta^2} + \frac{D_2}{D_1}\left(\frac{a}{b}\right)^4 \frac{\partial^4 w_{mn}}{\partial\eta^4}\right]$$

$$+ \left(1 + ig_m\right)\left(\frac{N_x a^2}{D_1}\,\frac{\partial^2 w_{mn}}{\partial\xi^2} + \frac{N_y a^4}{D_1 b^2}\,\frac{\partial^2 w_{mn}}{\partial\eta^2} + \frac{2N_{xy}a^3}{D_1 b}\,\frac{\partial^2 w_{mn}}{\partial\xi\,\partial\eta}\right)$$

$$+ \frac{\rho c a^4}{D_1}\,\alpha_{mn} w_{mn} + \frac{\gamma a^4}{D_1}\,\alpha_{mn}^2 w_{mn} = 0 \tag{6}$$

$$w_{mn}(\xi,0,t) = w_{mn}(\xi,1,t) = \frac{\partial^2 w_{mn}}{\partial\eta^2}(\xi,0,t) = \frac{\partial^2 w_{mn}}{\partial\eta^2}(\xi,1,t) = 0 \tag{7}$$

$$\left[\frac{\partial^3 w_{mn}}{\partial\xi^3} + \frac{\mu_y D_1 + 2D_{xy}}{D_1}\left(\frac{a}{b}\right)^2 \frac{\partial^3 w_{mn}}{\partial\eta^2\,\partial\xi} + \frac{N_x a^2}{D_1}\,\frac{\partial w_{mn}}{\partial\xi} \mp \bar{K}_d w_{mn}\right.$$

$$\left. \pm \bar{K}_t\left(\frac{a}{b}\right)^2 \frac{\partial^2 w_{mn}}{\partial\eta^2} + \frac{N_{xy}a^3}{D_1 b}\,\frac{\partial w_{mn}}{\partial\eta}\right]_{\xi=\pm\frac{1}{2}} = 0 \tag{8}$$

$$\left[\frac{\partial^2 w}{\partial\xi^2} + \mu_y\left(\frac{a}{b}\right)^2 \frac{\partial^2 w}{\partial\eta^2} \pm \bar{K}_r\,\frac{\partial w}{\partial\xi}\right]_{\xi=\pm\frac{1}{2}} = 0 \tag{9}$$

In equation (6), the structural damping has been included in the same manner as in reference 5 by multiplying each of the bending terms by $1 + ig_b$ and each of the membrane terms by $1 + ig_m$. The structural damping considered in this manner was shown in reference 6 to give good agreement with the experimental data. The spring constants have been nondimensionalized as follows:

$$\left.\begin{aligned} \overline{K}_d &= \frac{K_d a^3}{D_1} \\ \overline{K}_r &= \frac{K_r a}{D_1} \\ \overline{K}_t &= \frac{K_t a}{D_1} \end{aligned}\right\} \tag{10}$$

The inclusion of N_{xy} in equations (6) and (8) overly complicates the solution for natural modes and frequencies; therefore, these terms are omitted for simplicity. However, for the flutter solution, both N_{xy} terms (eqs. (6) and (8)) are included in the governing equation. (See the section entitled "Flutter Solution.") Equations (6) and (9), with $N_{xy} = 0$, are identical to those solved in reference 3 and the method of solution is discussed in detail therein.

Flutter Solution

A Galerkin-type flutter solution can be obtained using the natural mode shapes and frequencies and the following governing equation obtained from equation (4):

$$\int_{-1/2}^{1/2}\int_0^1 \left\{ \left(1 + ig_b\right)\left[\frac{\partial^4 w}{\partial \xi^4} + 2\,\frac{\mu_y D_1 + D_{xy}}{D_1}\,\frac{a^2}{b^2}\,\frac{\partial^4 w}{\partial \xi^2\,\partial \eta^2} + \frac{D_2}{D_1}\left(\frac{a}{b}\right)^4 \frac{\partial^4 w}{\partial \eta^4}\right] \right.$$

$$+ \left(1 + ig_m\right)\left[\frac{N_x a^2}{D_1}\,\frac{\partial^2 w}{\partial \xi^2} + \frac{N_y a^4}{D_1 b^2}\,\frac{\partial^2 w}{\partial \eta^2} + \frac{2N_{xy} a^3}{D_1 b}\,\frac{\partial^2 w}{\partial \xi\,\partial \eta}\right] + \frac{\gamma a^4}{D_1}\,\frac{\partial^2 w}{\partial t^2} + \frac{\rho c a^4}{D_1}\,\frac{\partial w}{\partial t}$$

$$\left. + \frac{2qa^3}{\beta D_1}\left[\cos\Lambda\,\frac{\partial w}{\partial \xi} + \frac{a}{b}\sin\Lambda\,\frac{\partial w}{\partial \eta}\right] \right\} d\xi\, d\eta - \int_0^1 \frac{N_{xy} a^3}{D_1 b}\,\frac{\partial w}{\partial \eta}\Bigg|_{-1/2}^{1/2} d\eta = 0 \tag{11}$$

The single integral term in the above expression is a boundary term and does not usually appear in the governing equation. However, since the mode shapes employed in the flutter solution are defined with $N_{xy} = 0$ (see section entitled "Vibration Solution"), they do not satisfy the boundary conditions of equation (8). Therefore, this term must be included as a part of the governing equation. (See ref. 7, p. 338.)

The flutter (eq. (11)) can be solved by assuming a solution in the form

$$w = \sum_{m=1}^{\infty} \sum_{n=1}^{\infty} A_{mn} w_{mn} e^{\alpha t} \tag{12}$$

where α is one of the complex frequencies. The flutter solution is obtained by substituting equation (12) into equation (11), with $w_{mn} = X_{mn} \sin n\pi\eta$, multiplying through by $X_{rs} \sin s\pi\eta$, and integrating over the total area. Performing the integration and rearranging the terms result in the following set of simultaneous equations:

$$A_{mn}\left[\frac{1}{\omega_r^2}\left(\alpha_{mn}^2 - \alpha^2\right) + \frac{g_a}{\omega_r}\left(\alpha_{mn} + \alpha\right)\right]$$

$$+ \frac{\lambda \cos \Lambda}{\pi^4} \sum_{r=1}^{\infty} A_{rn} \frac{Q_{mrns}}{P_{mrns}} + \frac{2\lambda a \sin \Lambda}{\pi^4 b} \sum_{s=1}^{\infty} A_{ms} \frac{\left[1 - (-1)^{s+n}\right]}{s^2 - n^2}$$

$$+ \frac{2\bar{K}_{xy}}{\pi^2} \frac{a}{b} \sum_{m=1}^{\infty} \sum_{n=1}^{\infty} \frac{A_{rs}}{P_{mrns}}\left(2Q_{mrns} - X_{mn}X_{rs}\right) \frac{ns\left[1 - (-1)^{s+n}\right]}{s^2 - n^2} = 0 \tag{13a}$$

where

$$Q_{mrns} = \int_{-1/2}^{1/2} \frac{\partial X_{mn}}{\partial \xi} X_{rs} \, d\xi \tag{13b}$$

$$P_{mrns} = \int_{-1/2}^{1/2} X_{mn} X_{rs} \, d\xi \tag{13c}$$

$$\omega_r^2 = \frac{\pi^4 D_1}{\gamma a^4} \tag{13d}$$

$$g_a = \frac{\rho c}{\gamma \omega_r} \tag{13e}$$

$$\overline{K}_{xy} = \frac{N_{xy}a^2}{D_1\pi^2} \tag{13f}$$

and

$$\lambda = \frac{2qa^3}{\beta D_1} \tag{13g}$$

For a nontrivial solution to equation (13a), the determinant of the coefficients of A_{mn} must equal zero. A standard eigenvalue routine for a square complex matrix is used to calculate the eigenvalues α of equation (13a); the values of α render the determinant equal to zero.

Flutter is considered to occur for the lowest value of the dynamic-pressure parameter λ for which the imaginary part of one of the frequencies is greater than zero (no damping) or vanishes (damping). Certain combinations or values of inplane loads (either N_x, N_y, and/or N_{xy}) result in the condition for some value of λ where both the real and the imaginary parts of the frequency vanish. This load condition is the buckling load in the presence of airflow for the panel.

RESULTS AND DISCUSSION

Range of Parameters

Solutions of the flutter determinant resulting from equation (13a) were obtained for isotropic panels ($D_1 = D_2 = D_{12}$) with various length-width ratios subjected to inplane shear loads. The length-width ratios were varied between 0.5 and 5.0 with combinations of inplane shear loads N_{xy} and inplane normal loads N_x between 0 and the buckling load. In order to keep the variables to a reasonable number, the inplane normal loads N_y, the rotational and torsional spring supports $\overline{K}_r$ and $\overline{K}_t$, respectively, and the flow angle Λ were set equal to zero for all calculations. Aerodynamic damping g_a and structural damping in bending g_b were varied over a realistic range. Membrane structural damping g_m was set equal to zero.

Convergence

Previous studies have shown that, for converged flutter solutions of unstressed panels, only one modal term is required in the cross-stream direction; the number of modal terms required in the flow direction depends on the panel orthotropy and the length-width ratio. However, when inplane shear loads are present, several modal terms are required in each direction. This is evident in figure 2 where sample convergence results are shown by plots of the dynamic-pressure parameter λ against the panel frequencies for simply

supported, isotropic panels with various inplane shear loads and for $a/b = 0.5$ and 2.0 (figs. 2(a) and 2(b), respectively). The peak of the frequency loop represents the critical value of λ for which flutter instability occurs. The data show large reductions in flutter stability with inplane shear loads; these reductions are discussed in more detail in the next section. The curves shown were calculated using ten modal terms in the streamwise direction and four modal terms (10,4) in the cross-stream direction. Also shown in figure 2 are the flutter values calculated using (4,4) modes, represented by the circle symbols, compared with values published in reference 2 (using (4,4) modes), represented by the cross symbols. The data indicate that, for $a/b = 0.5$ (see fig. 2(a)), converged solutions are obtained when using (4,4) modal terms; however, for $a/b = 2.0$ (see fig. 2(b)), (4,4) modal terms are not converged. Note in figure 2(b) that the flutter values calculated using (10,3) and (12,4) modal terms, represented by the square and diamond symbols, respectively, are essentially the same as the (10,4) results and so verify the convergence of the (10,4) mode solution. Similar data obtained for plates with an a/b up to 5 indicate that (10,4) modal terms in the analysis give converged solutions.

Effect of Inplane Shear

Flutter of simply supported panels.- The effect of inplane shear loads on the flutter of simply supported, isotropic panels may be seen in figure 3 where flutter boundaries are shown as a function of $\overline{K}_{xy}$ for a/b values of 0.5, 1.0, 2.0, 3.0, and 4.0. Calculations are made for the values of aerodynamic damping, $g_a = 0$ and $g_a = 0.1$, and of structural damping, $g_b = 0$ to $g_b = 0.05$. The termination point of the flutter boundaries, shown by the circular symbols, corresponds to the value of $\overline{K}_{xy}$ at which buckling occurs in the presence of airflow. The static buckling values of K_{xy} are also shown by the square symbols in figure 3, and are in agreement with the values presented in reference 8.

When the panel is loaded in inplane shear, the critical value of λ is lowered significantly below the value for zero stress. For $a/b = 3.0$ and $a/b = 4.0$ (see figs. 3(d) and 3(e)), certain values of $\overline{K}_{xy}$ near buckling result in an anomalous condition of flutter for zero velocity. This condition occurs for $g_a = g_b = 0$ and is a result of a shift in the order of the natural frequencies. The result is similar to the data shown in reference 5 for panels with inplane normal loads. Including the aerodynamic and the structural damping in the calculations removes the $\lambda = 0$ flutter condition. Usually the lowest two frequencies coalesce to define the flutter boundary. However, for certain values of $\overline{K}_{xy}$ and zero damping, the frequencies associated with the higher modes coalesce and result in unstable conditions which, subsequently, disappear as $\overline{K}_{xy}$ is either increased or decreased. Such higher mode flutter conditions were discussed in detail in reference 2 and were not considered valid flutter points. In addition, these higher mode flutter conditions can be removed by even a small amount of structural damping; therefore, they have been ignored in presenting the results contained herein.

Flutter of panels on deflectional supports.- The influence of deflectional spring supports on the flutter of square panels with inplane shear loads and with $g_a = 0.1$ and $g_b = 0.01$ may be seen in figure 4. In this figure, λ is shown as a function of $\bar{K}_{xy}$ for various values of $\bar{K}_d$, the nondimensional spring constant for uniform springs at the leading and trailing edges. (The $\bar{K}_d = 0$ represents free edges.) For small values of $\bar{K}_{xy}$, decreasing the spring stiffness $\bar{K}_d$ results in a large reduction in λ. Decreasing the $\bar{K}_d$ also results in a reduction of the buckling load with airflow. However, at the point of buckling, decreasing the $\bar{K}_d$ may result in either lower (destabilizing) or higher (stabilizing) values of λ.

Flutter of panels with inplane normal loads and shear loads.- The effects of inplane normal loads, in combination with shear, on the flutter of simply supported panels with $a/b = 1.0$ and $a/b = 4.0$ are shown in figures 5(a) and 5(b), respectively, where values of λ/λ_o are shown as a function of $\bar{K}_{xy}/\bar{K}_{xy_{bu}}$. (The term λ_o is the value of λ of the unstressed panel and $\bar{K}_{xy_{bu}}$ is the shear buckling value when $N_x = 0$ and with airflow.) Curves are presented for $g_a = 0.1$, $g_b = 0.01$, and for $N_x/N_{xy} = 0$, 0.7, 3.0, and 5.0. As can be seen, increasing the normal loads results in a more rapid reduction in λ/λ_o as $\bar{K}_{xy}/\bar{K}_{xy_{bu}}$ is increased. However, the minimum values of λ/λ_o, or the values of λ/λ_o at the point of buckling, are not changed significantly by inplane normal loads. This condition is in contrast to the flutter results obtained when N_y is added to panels loaded with N_x. (See ref. 9.) It should be noted that, for $a/b = 4.0$ (fig. 5(b)), the value of λ for flutter is a small percentage of λ_o for values of $\bar{K}_{xy}$ above 70 percent of the buckling value.

Flutter of Panels Loaded to Buckling

Flutter design curves for shear.- In the design of panels for flutter it is desirable to have solutions which are widely applicable and simple to use. Also, since the actual flight-load conditions may not be well known, the designer may prefer to design against the most critical flutter condition. For panels with inplane loads, the most severe flutter conditions have been shown in the preceding sections to occur at or near the point of buckling.

The flutter boundaries for isotropic panels at the point of buckling in shear are presented in figure 6 by the solid curves where values of λ are shown as a function of a/b for $g_b = 0.01$ and $g_b = 0.04$. The flutter boundaries do not vary monotonically with a/b for small values of a/b and g_b but do, or tend to do so, as a/b or g_b is increased. Although the flutter boundaries given by the solid curves in figure 6 may be used as a conservative design criteria, more simplified curves may be defined by the minimum points of the actual flutter boundaries such as shown by the dashed curves in

figure 6. Although these curves are more conservative than necessary for certain values of a/b (near 1.25 and 2.75 for $g_b = 0.01$), their simplicity should justify their use in most practical design applications.

Design curves similar to the dashed curves in figure 6 have been defined for several values of g_b and are presented in figure 7 by the solid curves, where λ is shown as a function of a/b on a logarithmic scale. The resulting shear-load design curves are nearly parallel and, for $a/b \geq 2.0$ and $g_b \geq 0.01$, they are a family of straight lines that may be approximated by the equation

$$\lambda = 380 g_b \left(\frac{a}{b}\right)^{2.6} \tag{14}$$

For $a/b \leq 2.0$, the above equation may be more conservative than necessary. For $g_b \leq 0.01$, the design curves defined as above are so restrictive that flutter boundaries similar to the solid curves in figure 6 will probably need to be used.

The design curves obtained from reference 10 for simply supported, isotropic plates with inplane normal loads are also shown in figure 7 by long dashed curves. The normal-load design curves (see ref. 10) were developed with a/b values up to 10.0, whereas the shear-load design curves were developed with values of $a/b \leq 5.0$. Because of the large number of modal terms required for converged flutter solutions when shear loads are included, it is impractical to obtain flutter boundaries for a/b values much above 5.0. However, because of the similarity of the shear-load and normal-load design curves, it seems reasonable to expect the shear design curves to be valid for values of a/b to 10.

Although the normal and shear-load design curves show almost identical variations with a/b, the panels subjected to normal buckling loads will flutter at a lower value of λ than will the same panels subjected to shear buckling loads. Also, the panels subjected to a combination of inplane shear and normal loads up to the point of buckling were shown (see the section entitled "Flutter of panels with inplane normal loads and shear loads") to experience flutter at approximately the same value of λ as do the panels subjected to shear buckling loads only. Thus, the normal-load design curves can be conservatively used for applications involving either inplane shear or normal loads or combinations of these loads.

The flutter design curves for shear loading and for $g_b = 0.01$ are presented in a different form in figure 8 where $q/\beta E$ is shown as a function of h/b for panels with various length-width ratios. The shear design curves are extended to $a/b = 10.0$ by the approximate equation (14) and are shown by the dashed lines in figure 8. The resulting curves show the effect that the panel dimensions have on the flutter speed. Increasing the panel thickness h/b and decreasing the length-width ratio a/b both result in an increase in the flutter speed. For thin panels (h/b small), the panel length-width

ratio a/b has very little effect on the flutter speed. For thick panels (large h/b), increasing the panel length-width ratio results in a substantial reduction in the flutter speed.

Application of shear design curves.- One of the early shuttle cargo-bay door designs consists of a thin aluminum skin reinforced with hat-section stiffeners, the details of which are shown in figure 9. The stiffeners were spaced 13.2 cm (5.2 in.) apart parallel to the flow; they terminate at frames spaced 58.4 cm (23 in.) apart transverse to the flow. The aluminum skin, which is 0.076 cm (0.030 in.) thick, is covered externally with an insulation material (not shown) for thermal protection during reentry. The most critical period of shuttle flight for panel flutter occurs during ascent when the door has high torque loads which, for the early design, cause local shear buckling in the thin aluminum skin. For flutter calculations the effect of curvature should be small and the possible beneficial effects of the external insulation are neglected. Thus, consider the skin between stiffeners as an isotropic flat plate simply supported on all edges with $a/b = 8.84$ and $h/b = 0.012$. For these values, the curves in figure 8 give values of $q/\beta E$ of approximately 12×10^{-8} or a value of q/β for aluminum of approximately 8.6 kPa (180 psf). Since the shuttle may experience values of q/β up to 48 kPa (1000 psf), local panel flutter could occur on a door surface with this design for inplane shear loads up to the point of buckling. If h/b is doubled without changing the value of a/b, q/β for flutter would be increased by almost a factor of 8, which would provide an ample flutter margin.

CONCLUDING REMARKS

A modal flutter analysis for biaxially loaded, orthotropic panels using linear piston-theory aerodynamics has been extended in order to include the effects of inplane shear loading. Flutter boundaries for shear loads up to buckling are calculated for simply supported, isotropic panels of various length-width ratios and for a square, isotropic panel with elastic boundary conditions along the leading and trailing edges.

Convergence studies for panels with inplane shear showed that several modal terms are required in the cross-stream direction as well as in the streamwise direction. Thus, a large total number of modal terms are required for convergence. For panels with aspect ratios above 5.0, the number becomes so large that flutter calculations by the normal-mode method are impractical.

For simply supported, isotropic plates, inplane shear loads have large destabilizing effects and, when loaded to buckling, may reduce the flutter dynamic pressure by approximately the same amount as inplane normal buckling loads. Deflectional springs on the leading and trailing edges have a large destabilizing influence on the flutter of unstressed panels, but at the point of buckling the springs may be either stabilizing or destabilizing.

Flutter design curves were developed for panels loaded to buckling in shear. These curves show the flutter dynamic pressure, for panels with length-width ratios above 2.0, to be directly proportional to the structural damping and to the panel length-width ratio to the 2.6 power. Flutter design curves for buckling in inplane shear or combinations of inplane shear and normal loads were found to be conservatively predicted by the design curves for panels buckled under inplane load N_x alone. Calculations made for an early proposed design of the shuttle cargo-bay door indicate that practical panels, which have otherwise been adequately designed, could become flutter critical if inplane shear loads approach the buckling value.

Langley Research Center,
National Aeronautics and Space Administration,
Hampton, Va., January 22, 1975.

REFERENCES

1. Anon.: Panel Flutter: NASA Space Vehicle Design Criteria (Structures). NASA SP-8004, 1964. (Revised 1972.)

2. Eisley, J. G.; and Luessen, G.: The Flutter of Thin Plates Under Combined Shear and Normal Edge Forces Including the Effects of Varying Sweepback. Paper No. 62-90, Inst. Aerospace Sci., June 1962.

3. Sawyer, James Wayne: Flutter of Elastically Supported Orthotropic Panels Including the Effects of Flow Angle. NASA TN D-7491, 1974.

4. Libove, Charles; and Batdorf, S. B.: A General Small-Deflection Theory for Flat Sandwich Plates. NACA Rep. 899, 1948. (Supersedes NACA TN 1526.)

5. Shore, Charles P.: Effects of Structural Damping on Flutter of Stressed Panels. NASA TN D-4990, 1969.

6. Heard, Walter L., Jr.; and Bohon, Herman L.: Natural Vibration and Flutter of Elastically Supported Corrugation-Stiffened Panels – Experiment and Theory. NASA TN D-5986, 1970.

7. Fung, Y. C.: Foundations of Solid Mechanics. Prentice-Hall, Inc., 1965, pp. 338-339.

8. Stein, Manuel; and Neff, John: Buckling Stresses of Simply Supported Rectangular Flat Plates in Shear. NACA TN 1222, 1947.

9. Bohon, Herman L.: Flutter of Flat Rectangular Orthotropic Panels With Biaxial Loading and Arbitrary Flow Direction. NASA TN D-1949, 1963.

10. Shore, Charles P.: Flutter Design Charts for Biaxially Loaded Isotropic Panels. J. Aircraft, vol. 1, no. 4, July-Aug. 1970, pp. 325-329.

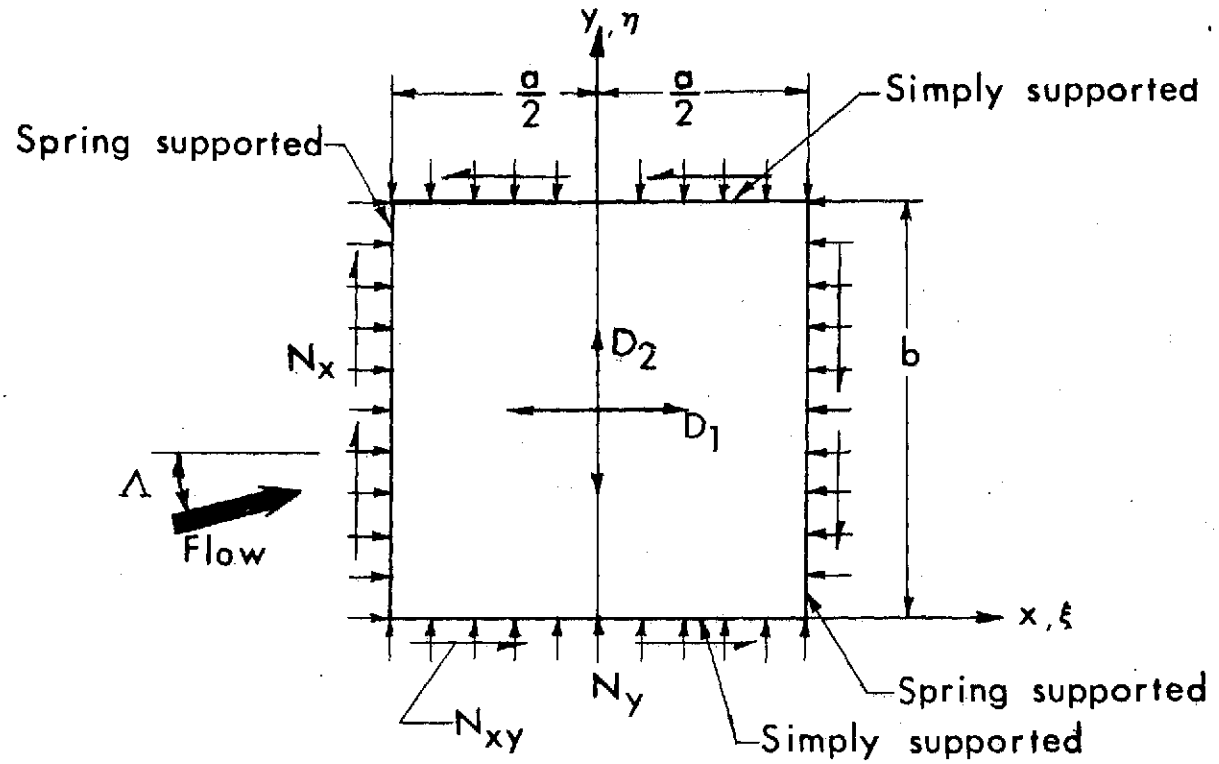

Figure 1.- Panel geometry and coordinate system.

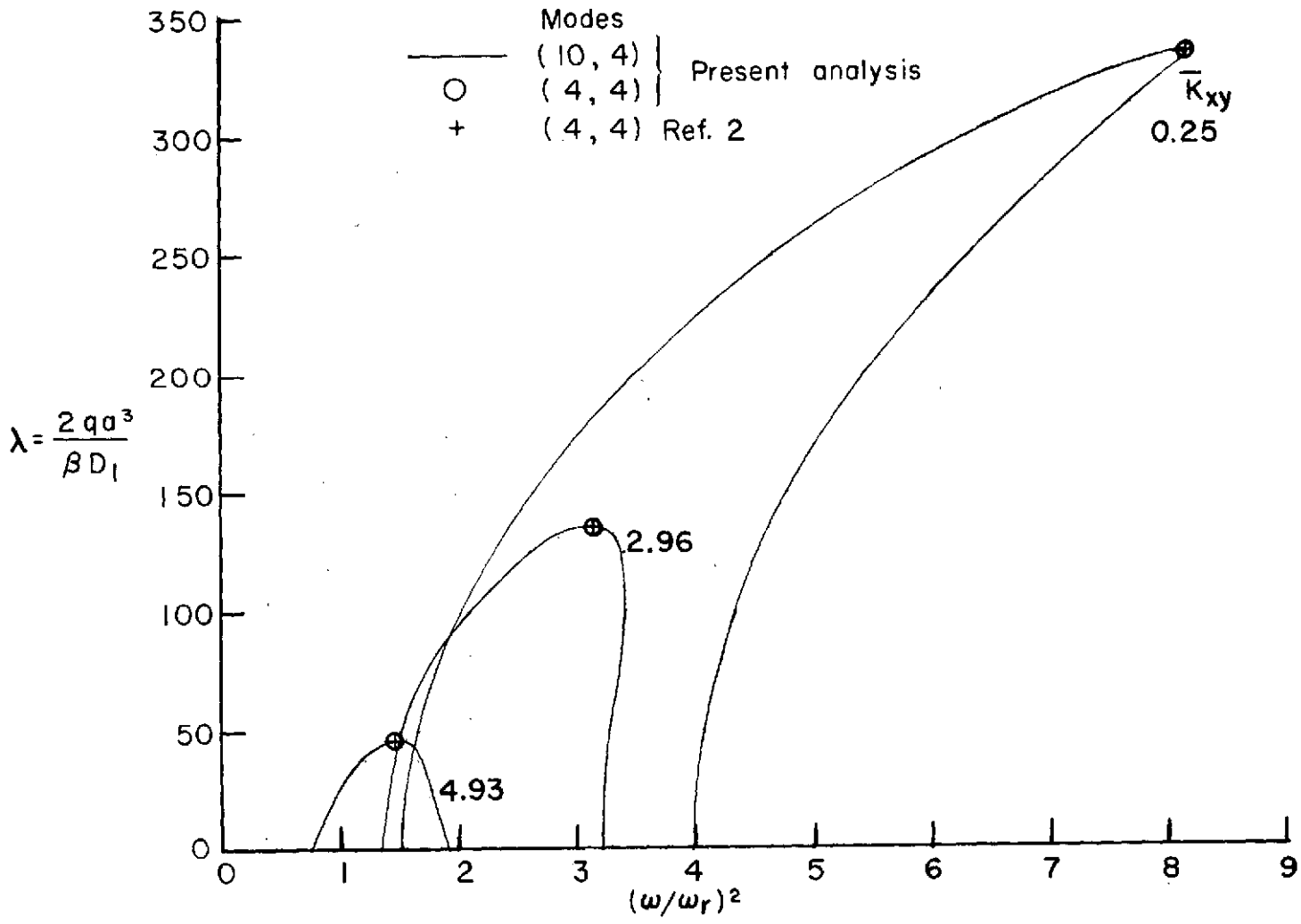

(a) a/b = 0.5.

Figure 2.- Convergence at point of coalescence of modal analysis with inplane shear $g_a = g_b = 0$.

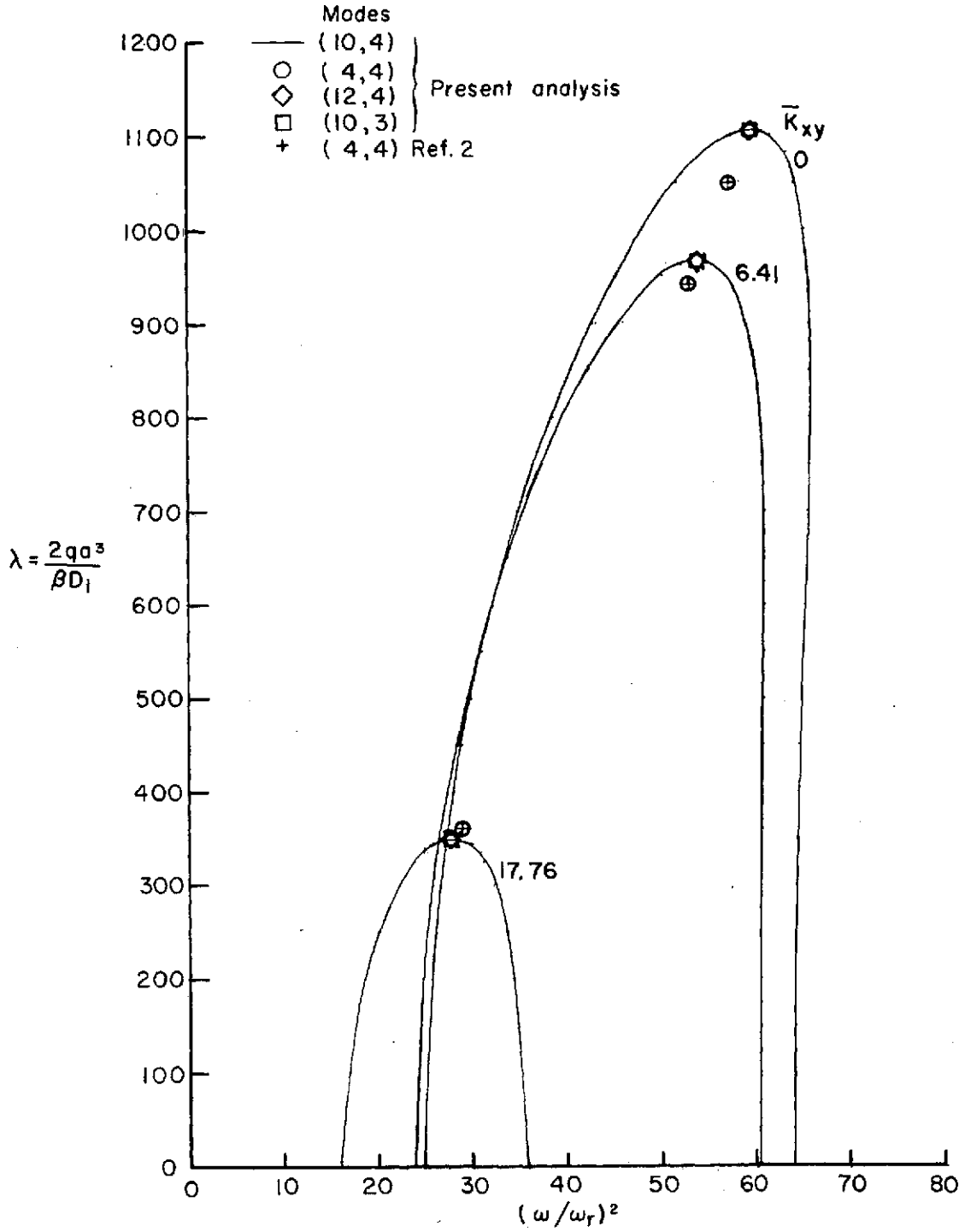

(b) a/b = 2.0.

Figure 2.- Concluded.

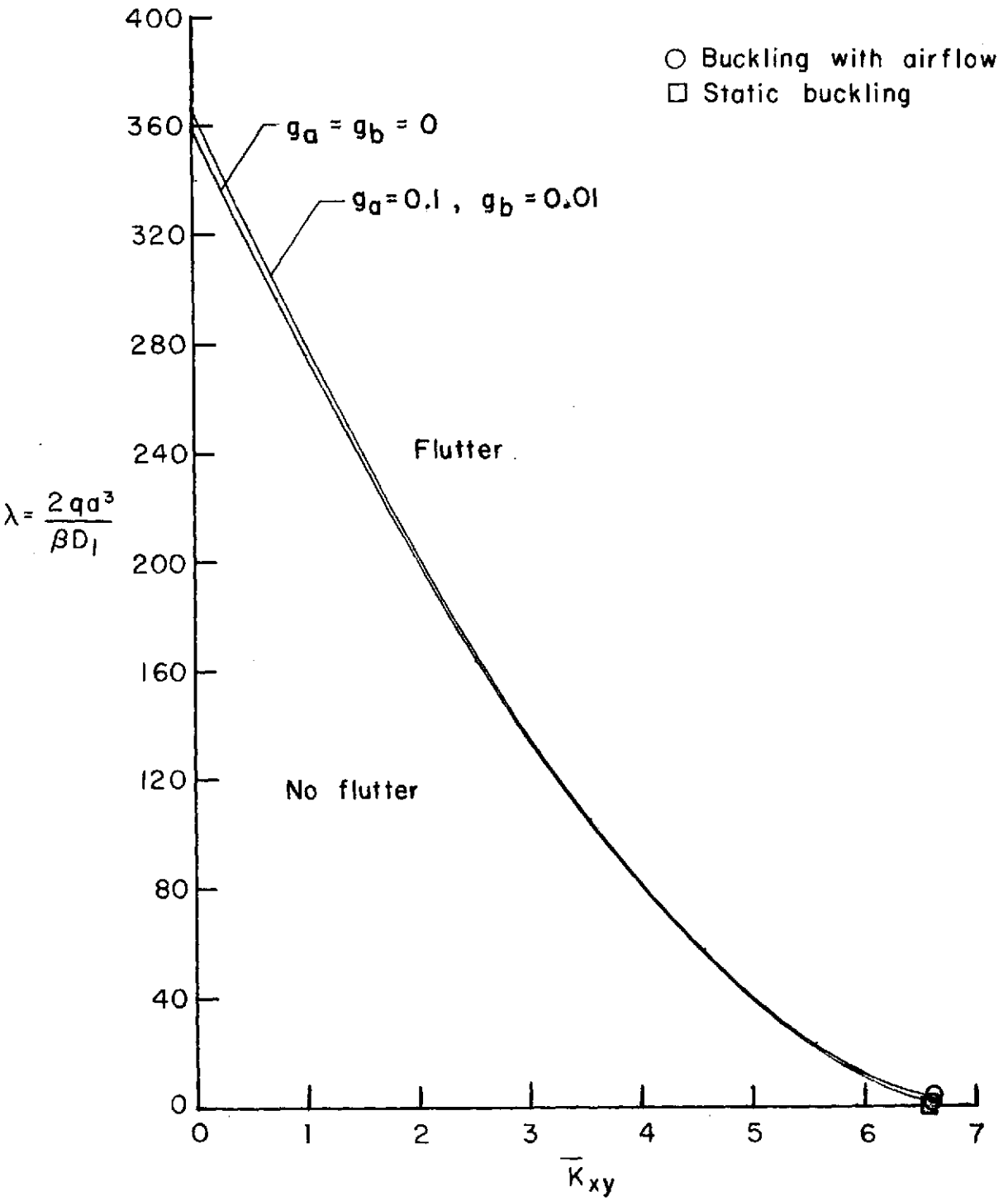

(a) a/b = 0.5.

Figure 3.- Flutter boundaries for simply supported, isotropic panels with inplane shear.

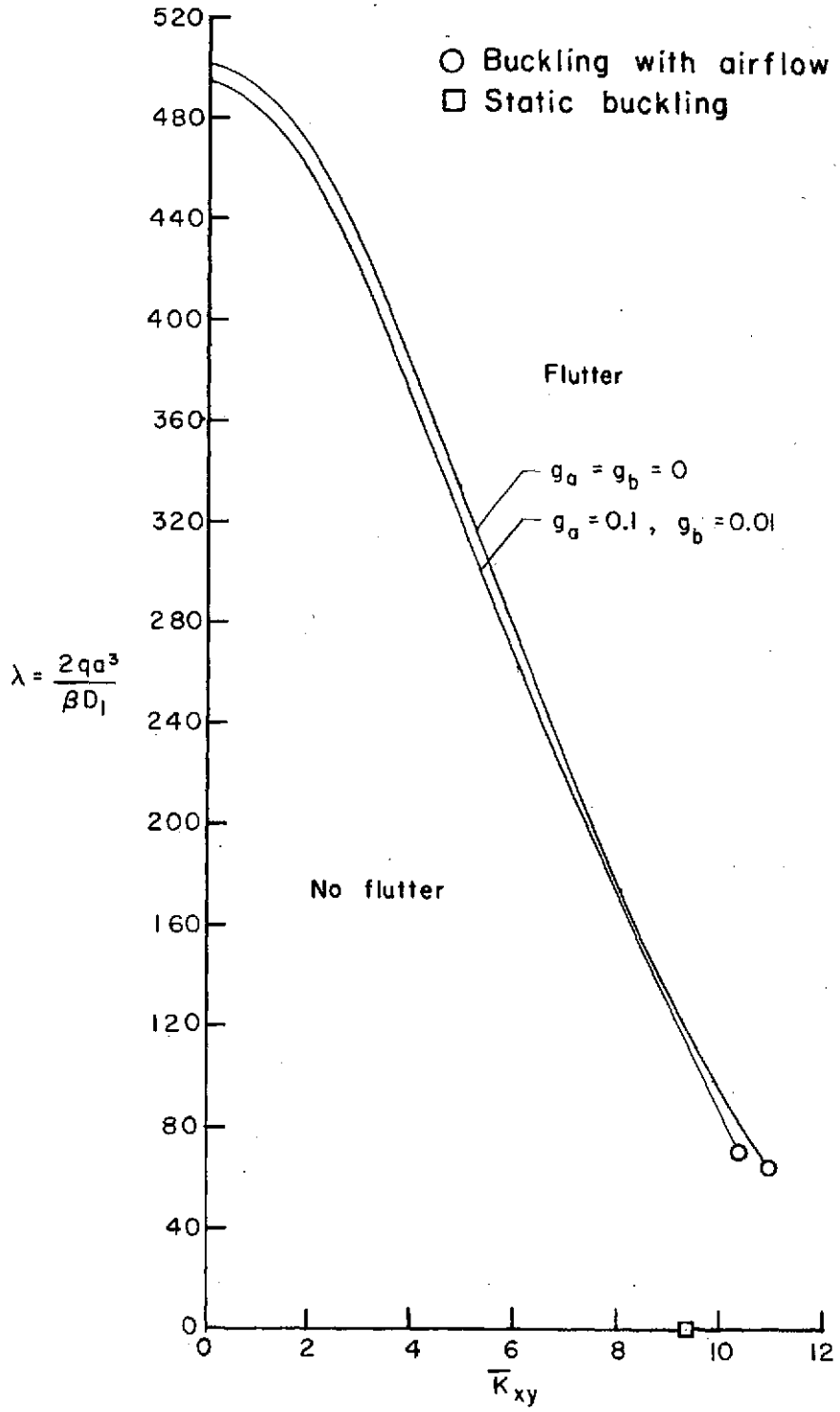

(b) a/b = 1.0.

Figure 3.- Continued.

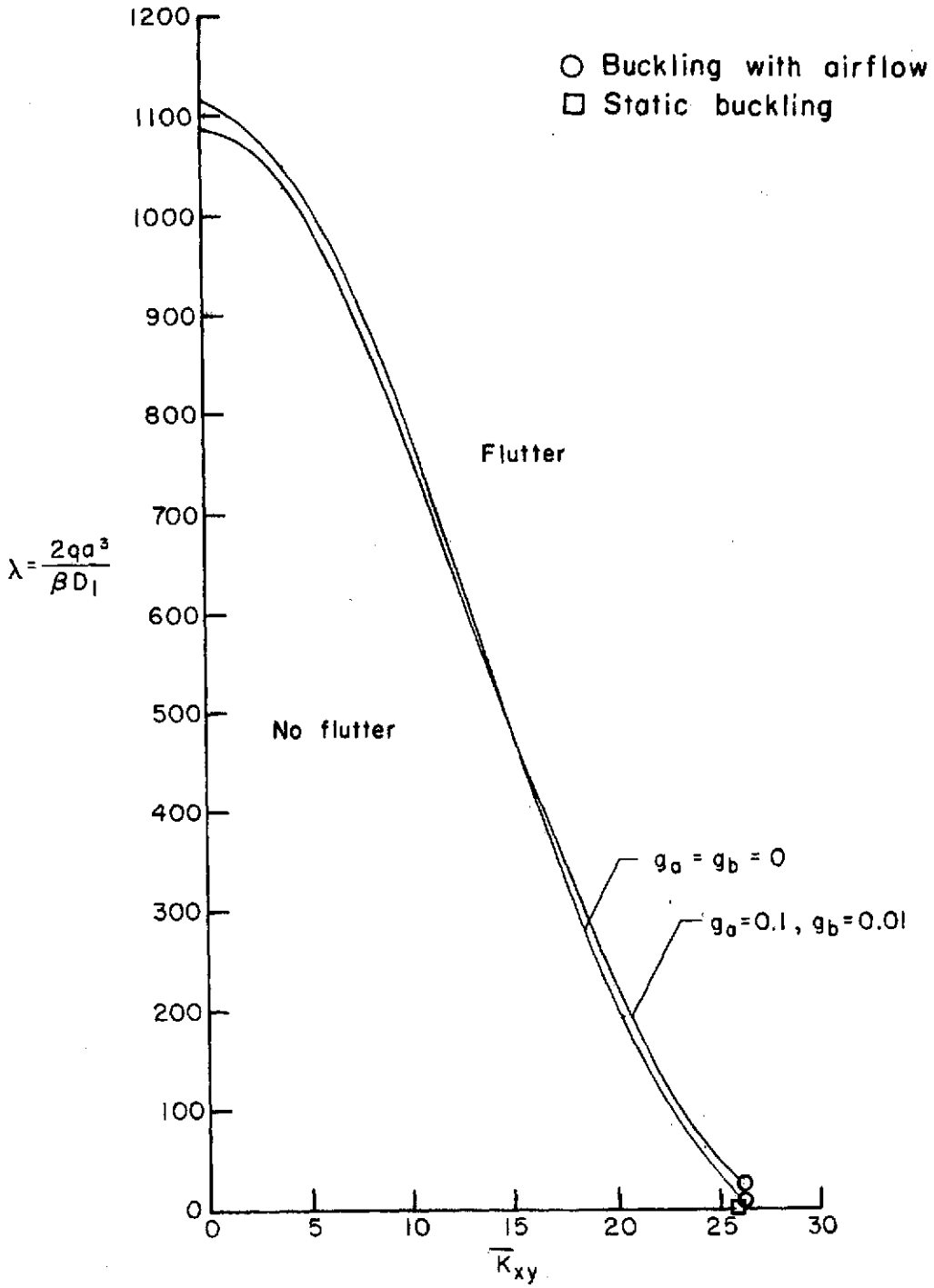

(c) a/b = 2.0.

Figure 3.- Continued.

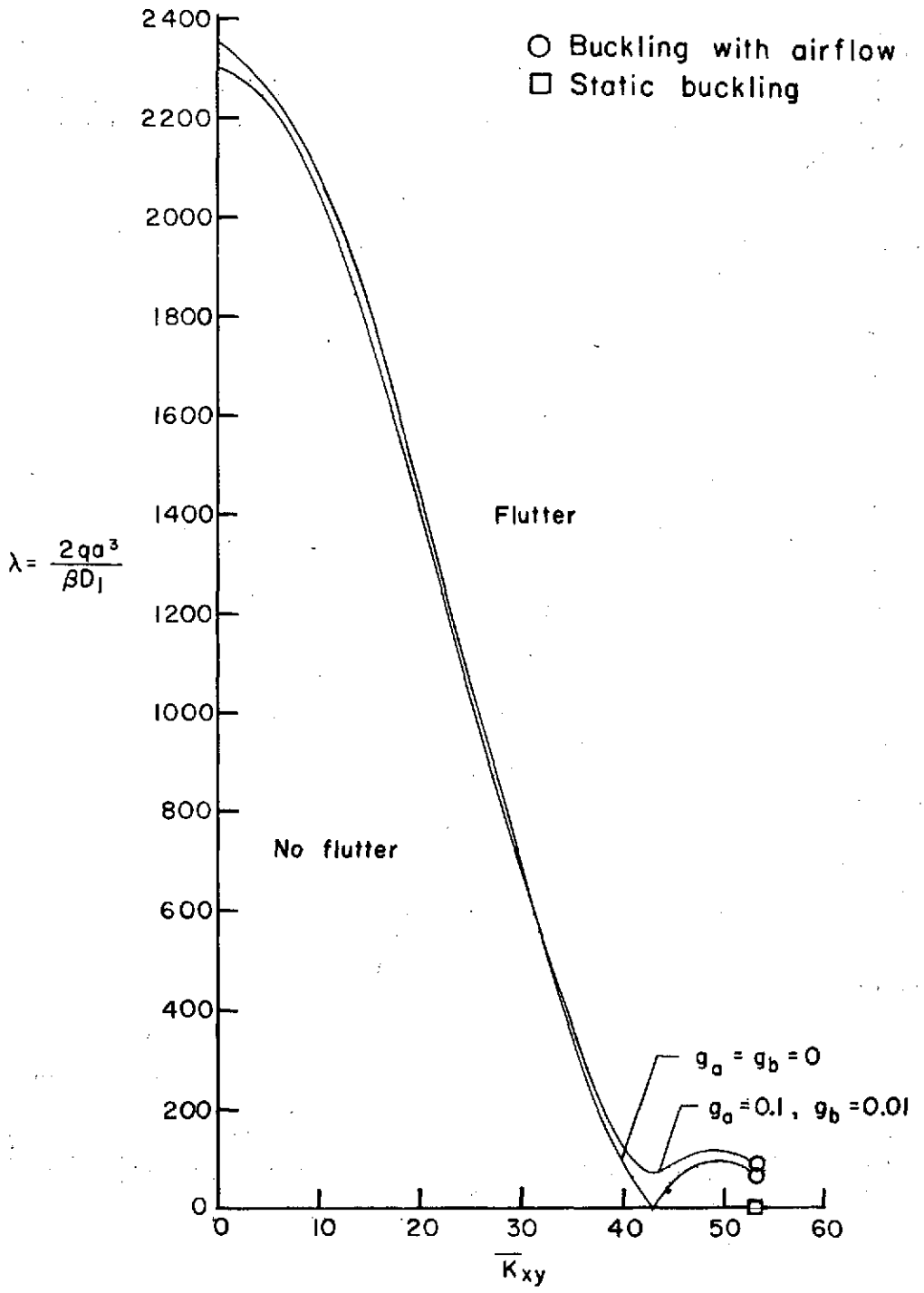

(d) a/b = 3.0.

Figure 3.- Continued.

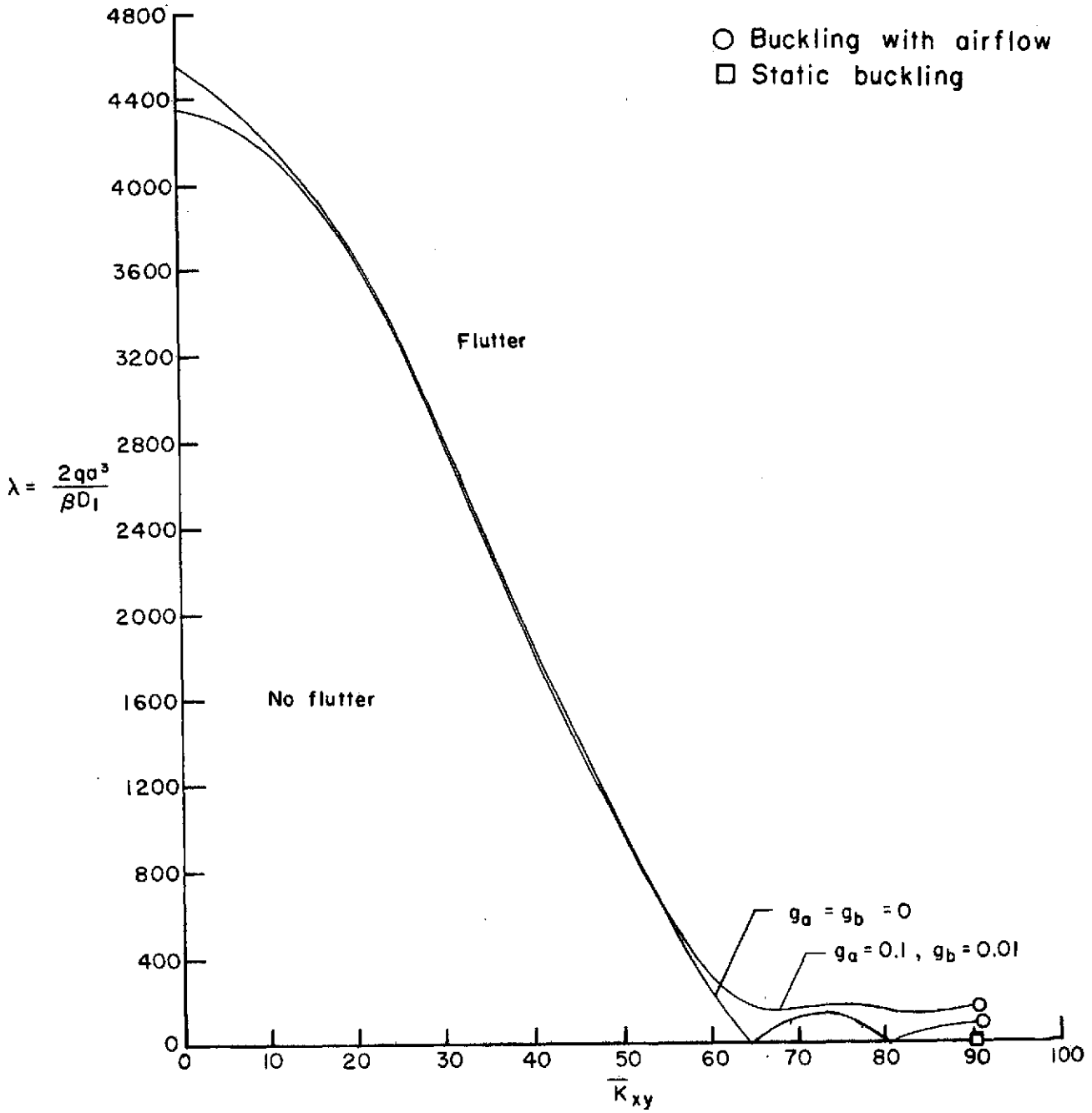

(e) a/b = 4.0.

Figure 3.- Concluded.

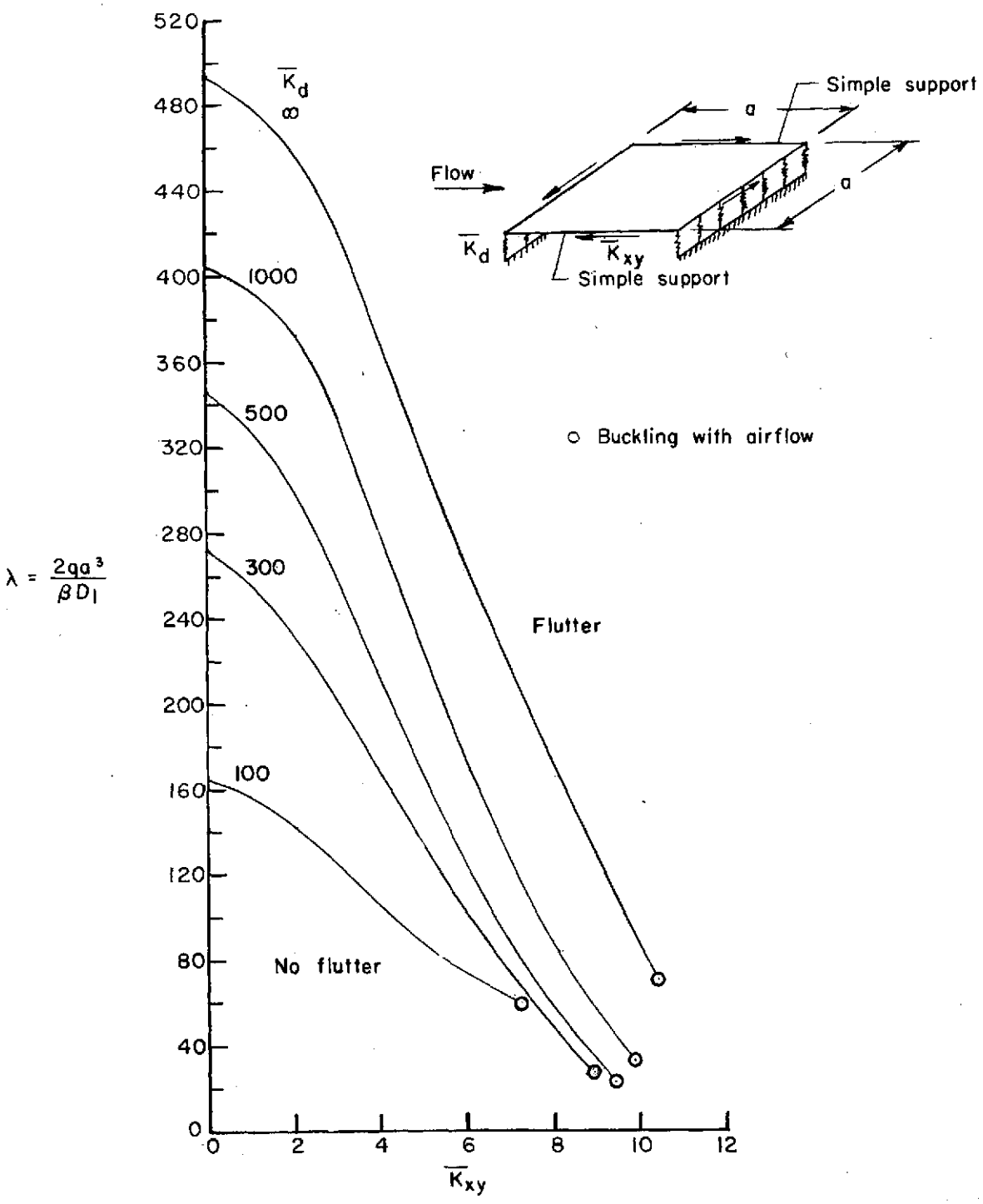

Figure 4.- Effect of leading- and trailing-edge deflectional spring supports on flutter boundaries for square panels with inplane shear $g_b = 0.01$; $g_a = 0.1$.

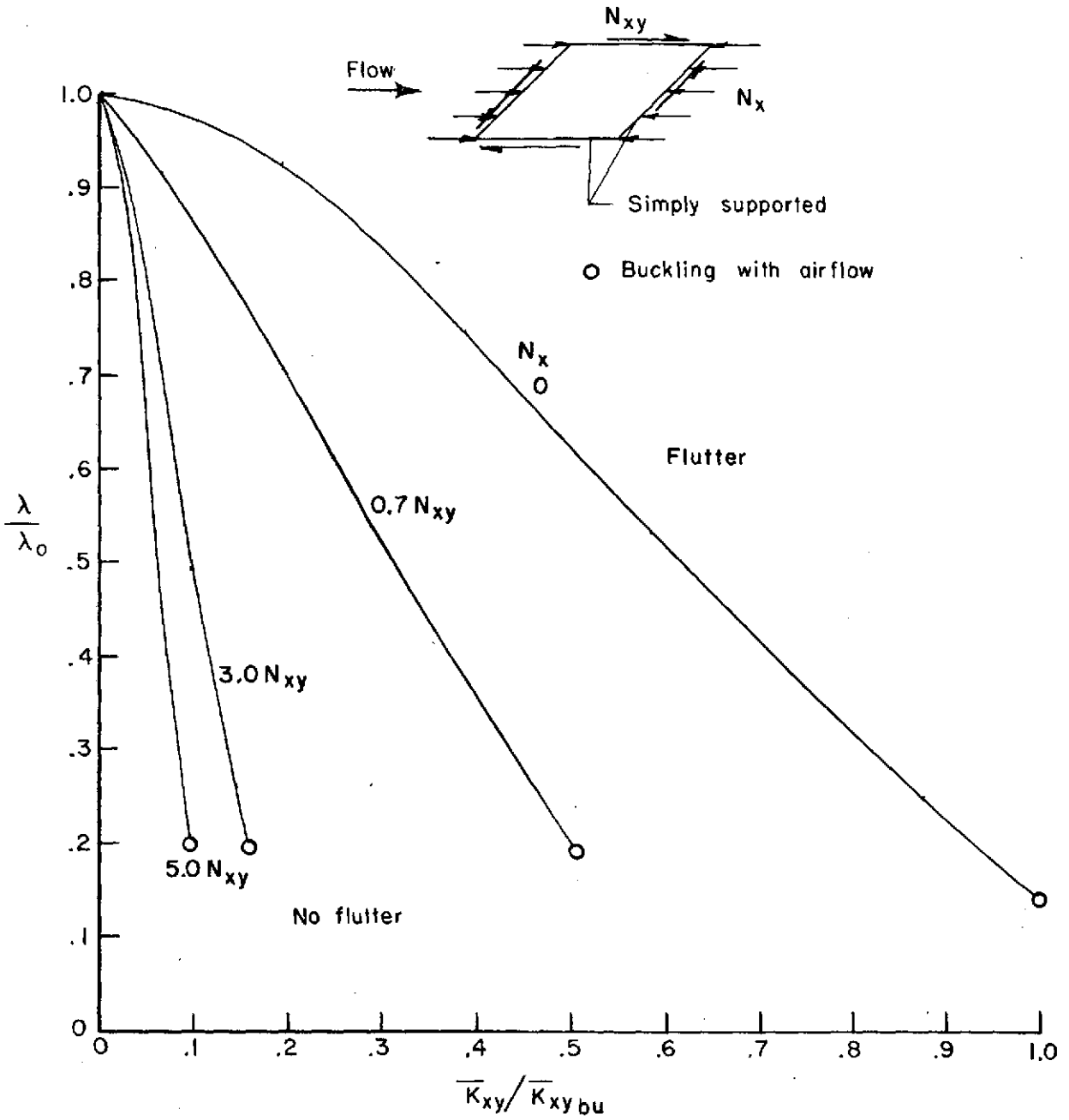

(a) a/b = 1.0.

Figure 5.- Flutter boundaries for simply supported, isotropic panels with inplane shear and normal loads. $N_y/N_{xy} = 0$; $g_a = 0.1$; and $g_b = 0.01$.

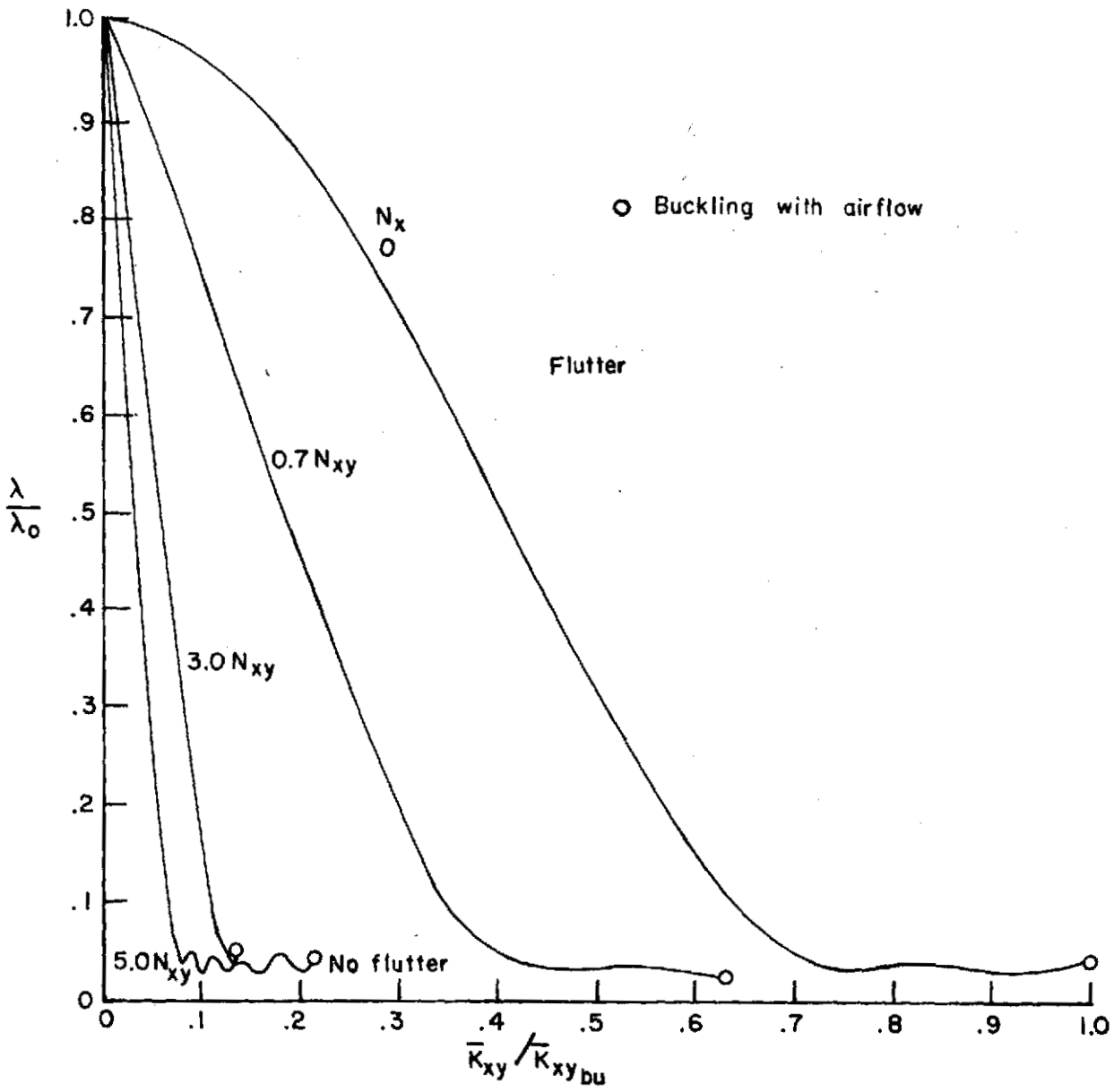

(b) a/b = 4.0.

Figure 5.- Concluded.

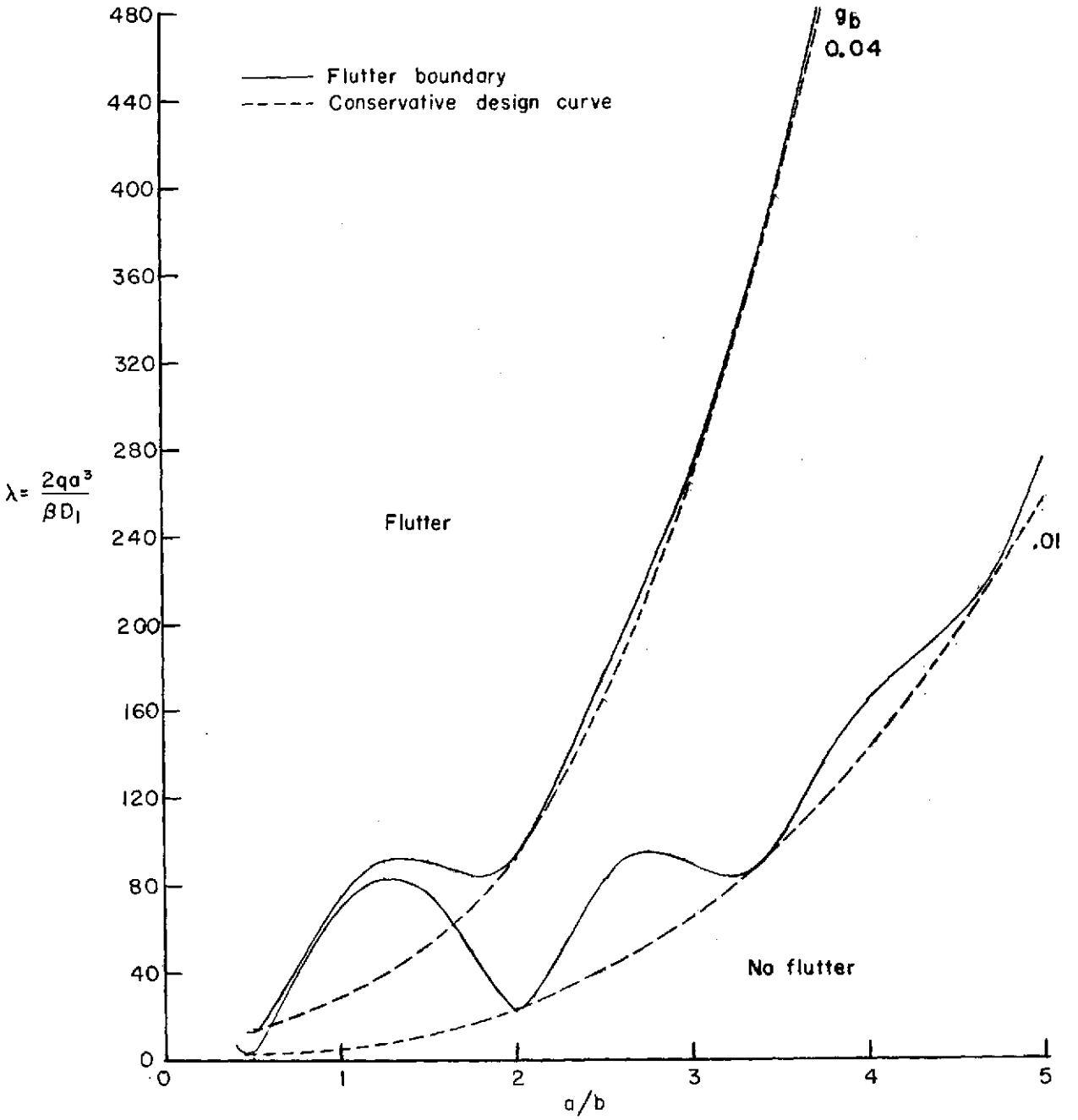

Figure 6.- Influence of length-width ratio on flutter of simply supported, isotropic panels loaded to buckling in inplane shear.

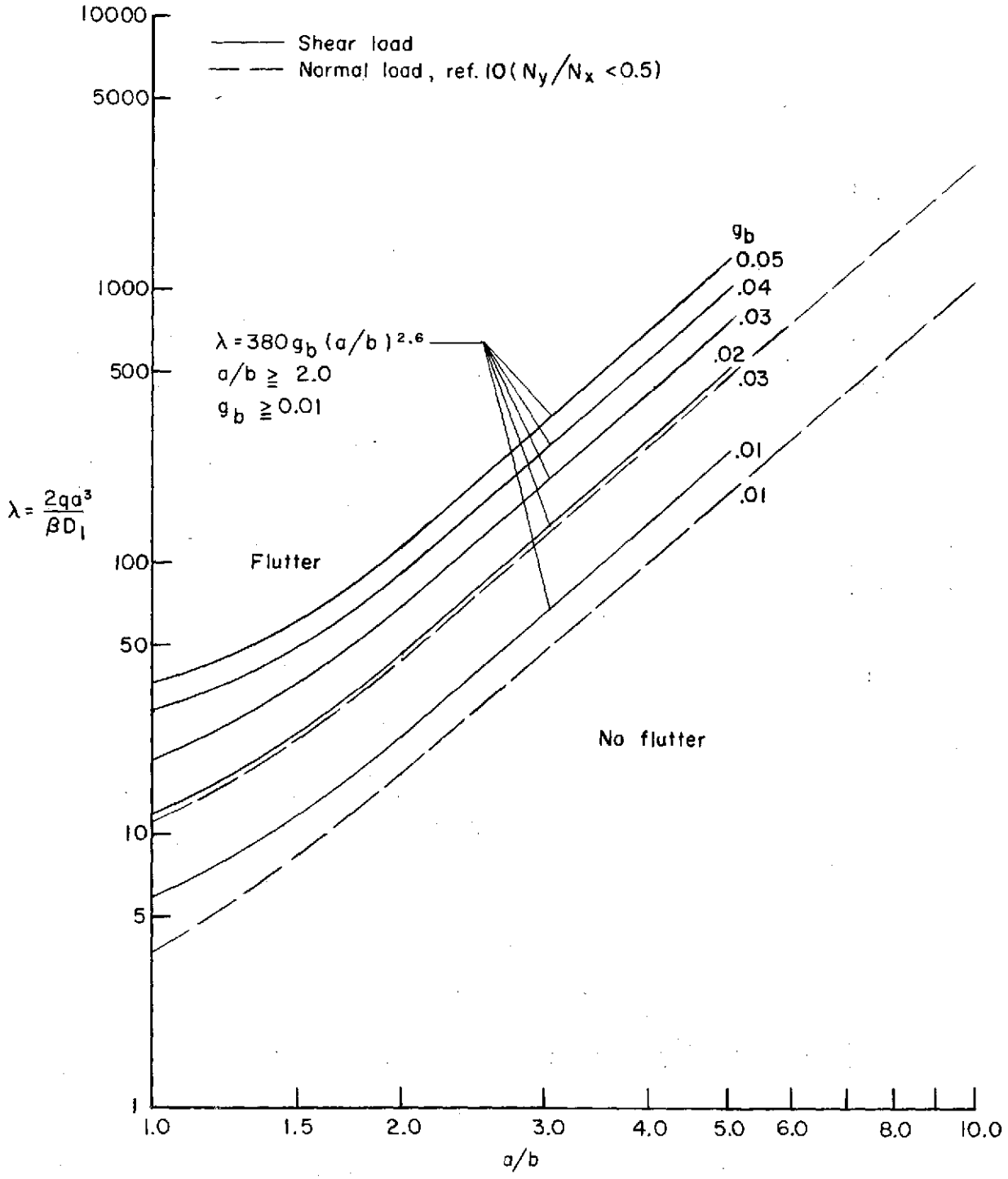

Figure 7.- Flutter design curves for simply supported, isotropic panels loaded to buckling.

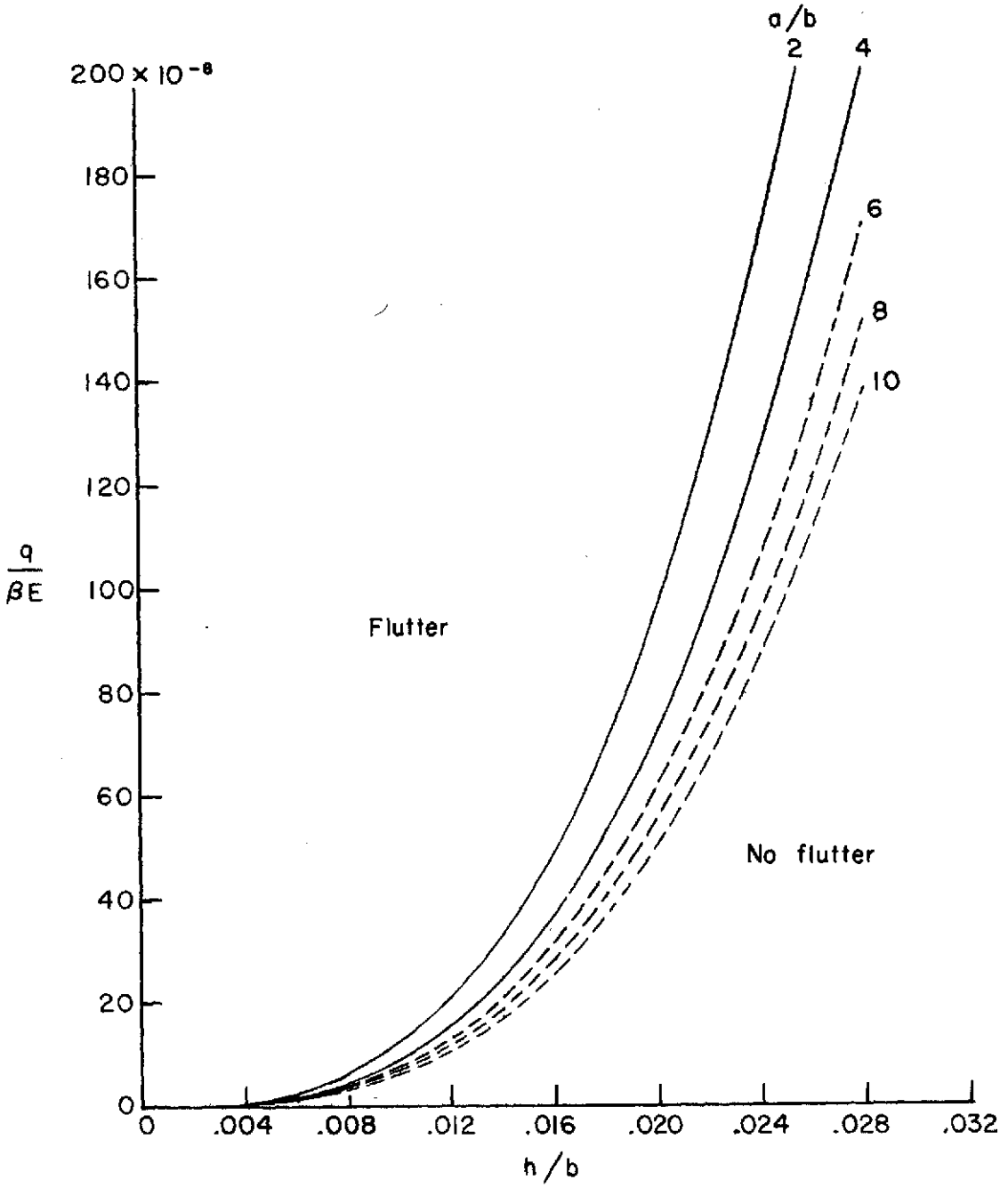

Figure 8.- Flutter design curves for simply supported, isotropic panels loaded to buckling in shear as a function of panel geometry. $g_b = 0.01$.

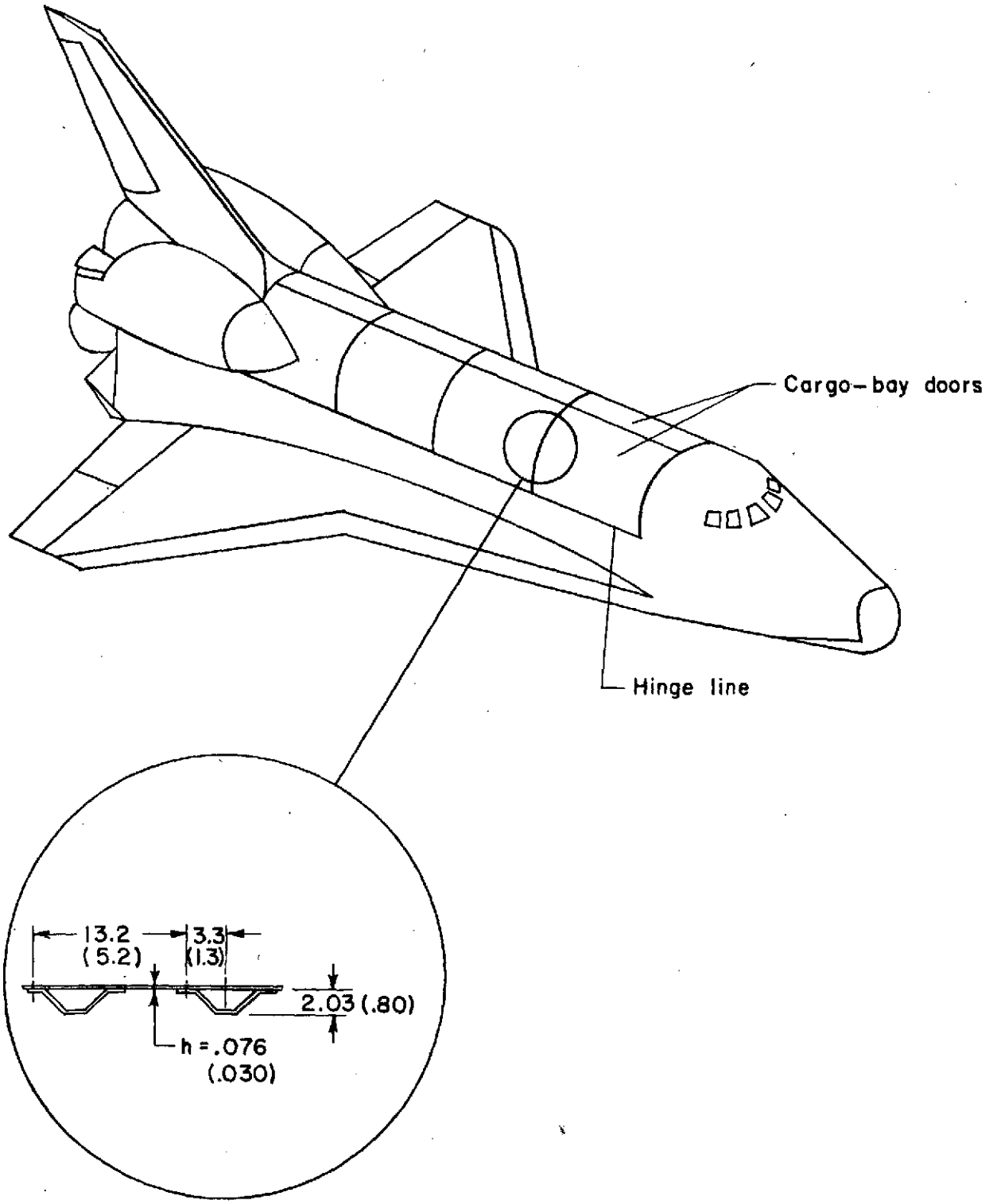

Figure 9.- Detail sketch of one of the early shuttle cargo-bay door designs.